Signal Processing and Renewable Energy
September 2023, (pp. 77-93)
ISSN: 2588-7327
eISSN: 2588-7335

Perturb and Observe Maximum Power Point Tracking Method Based on Estimation of Irradiation Change by Independent Component Analysis

Sonya Nodehi [1], Mazdak Teimoortashloo [2*]

[1] Bojnourd Branch, Islamic Azad University, Bojnourd, Iran.
[2] Electrical Industry Technology Development Research Center, Bojnourd Branch, Islamic Azad University, Bojnourd, Iran

Received: 16-Aug-2023, Revised: 12-Sep-2023, Accepted: 13-Sep-2023.

Abstract

The techniques of maximum power point tracking (MPPT) are used for maximizing the output of PVs by continuously tracking the maximum power point (MPP) of their P-V curves, which depend both on the panel temperature and the input insolation. Various MPPT algorithms have been studied in papers. One of the popular methods is the Perturb and Observe (P&O) method. The P&O method has a special place due to its simplicity and low running cost. However, one of the disadvantages of this method is the failure to track MPP under fast-changing irradiation. In this paper, the scale of the changing irradiance signal is extracted without the need for an irradiance sensor by an independent component analysis (ICA) algorithm, and then, according to this estimation and P&O method, a new algorithm is proposed. The simulation results show, in the case of constant temperature and fast increasing of irradiation and different locations of the initial operating point, the proposed method performance is better than the former P&O in the tracking of maximum power point.

Keywords: Maximum Power Point Tracking, Independent Component Analysis, Photovoltaic, Perturb and Observe, Irradiance.

1. INTRODUCTION

The increasing demand for energy from all over the world and depletion of conventional energy resources, as well as their undesirable impact on the environment like releasing greenhouse gases and then increasing global warming has made the researchers develop a new solution for producing energy.

*Corresponding Authors Email: mazdak1978@yahoo.com

Considering all these factors renewable energy is one of the best solutions [1]. Among renewable resources energy such as wind, tidal, geothermal, and others, solar energy is considered one of the most useful sources, due to its sustainability, local availability, cleanliness, and a suitable choice for a variety of applications mainly due to the possibility of direct conversion of this form of energy to electrical energy using PV systems [2 -6]. However, PV systems suffer from low efficiency because of their dependence on weather conditions such as temperature and irradiance, also I-V and P-V curves of PV systems typically show non-linear behavior. The I-V and P-V curves have a unique maximum power point, at which the PV system operates with the maximum output at the highest efficiency. So, to maximize the efficiency of PV panels, maximum power point tracking methods are used in PV systems [7 -8]. The task of MPPT is to set the system operating point near the MPP under different atmospheric conditions, and so far various methods have been proposed such as perturb and Observe (P&O), Incremental Conductance (Inc-Con), Short Circuit Current (SCC), Open Circuit Voltage (OCV), Artificial Neural Network (ANN), Fuzzy Logic Controller, etc. Among all these methods P&O is the most popular way, but tracking the MPP under fast-changing of irradiation is poorly performing [9]. To overcome this problem, some solutions have been reported up to now such as drift modified P&O [10], which was proposed to capture the MPP properly under increasing solar irradiation. The change in the module current (ΔI) is considered in addition to the change in power (ΔP) and the change in the voltage (ΔV) to track properly the MPP. The drift modified method tracks properly the MPP only both the changes (ΔV) and (ΔI) are positive. A modified P&O technique was proposed by [11] to ensure that MPP tracking of the classical P&O remains in the correct direction even under rapidly varying irradiance conditions. In this technique, the sign of voltage perturbation (ΔV) was considered the sign of change in the voltage (ΔV) and power (ΔP) multiplied together. This resulted in reducing oscillations around MPP at slightly improving the tracking speed with no improvement of the average efficiency under dynamic irradiation conditions [11]. The Voltage-Hold Perturbation and Observation method was proposed for tracking the maximum power point during irradiation changes. A capacitance is connected in parallel with the PV array. The capacitor voltage is related to the increase/decrease of the generated PV current being dependent on the solar irradiation level. The VH-P&O algorithm stops the classical perturbation process during the irradiance changes and holds the reference voltage at the PV capacitor voltage. As soon as the irradiation change stops, the MPP is determined using the classical P&O method with decreasing step size. The method has a large oscillation around MPP like the classical one as well and its tracking speed is equal to that of the classical P&O method [12].

This paper introduces a solution to investigate the solar irradiation change without the need for an irradiation sensor, which helps classical P&O to have better performance in case of constant temperature and increasing irradiation. Section 2 presents

the PV system model and classical Perturb and Observe method. Section 3 is about the independent component analysis concept and Algorithm. The proposed method and details about it are elaborated in section 4. Simulation and results are carried out in section 5. Finally, section 6 presents the conclusion.

2. INVESTIGATED PV SYSTEM AND PERTURB AND OBSERVE

The PV system proposed in this paper consists of a PV module, a DC-DC voltage converter, and a resistive load. The module parameters including short-circuit current I_{SC}, open-circuit voltage V_{OC}, and I_{MPP}, V_{MPP}, and P_{MPP} are current, voltage, and power at the maximum power point respectively. DC-DC voltage converters are used for matching the characteristics of the load with solar panels [2].

The most popular and simple model used to represent the PV cell is the single-diode model. It is composed of series and parallel resistors connected to a diode and a current source as shown in Figure 1.

R_P represents the loss in which a small leakage current flows through the parallel path (High-value order of kΩ). R_S represents the losses which are a loss of metal grid (about 1 Ω). The equations for an output current of the solar cell.

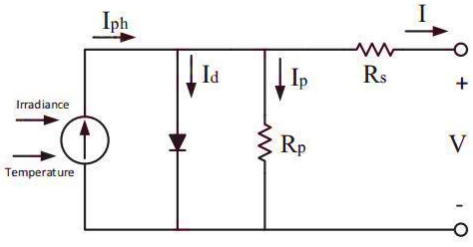

Fig. 1. Single diode equivalent circuit of the solar cell [7].

$$I = I_{ph} - I_d - I_p \quad (1)$$

Where the I represents output current, I_{ph} is photovoltaic current without loss and this current depends on irradiance and the temperature of the solar cell, I_d is the current through the diode, and I_p is the current leakage in parallel resistance.

The amount of power obtained from a single solar cell is extremely low, to obtain desired power, the solar cells are connected in series to create PV panels, and PV panels can be connected in series or parallel to create PV arrays [13].

Another condition for transferring maximum power to the load is that the load resistance is equal to the resistance of the other parts of the circuit. The internal resistance of the panels, which is obtained by dividing the output panel voltage by its current, will be a variable parameter that depends on factors such as irradiation level and temperature. If this resistance is more or less than the load resistance, the efficiency of the panels will be reduced. Since we do not have control over the size of the load, adjusting the impedance is done by adjusting the duty cycle of the converter (D). The four most common types of DC to DC converters used for this purpose are the buck converter, boost converter, buck-boost converter, and cuck converter. The selection of the type of dc-dc voltage converter depends on the voltage involved. Since the output voltage of the module is usually low to apply to load, the boost converter is required to amplify it [7].

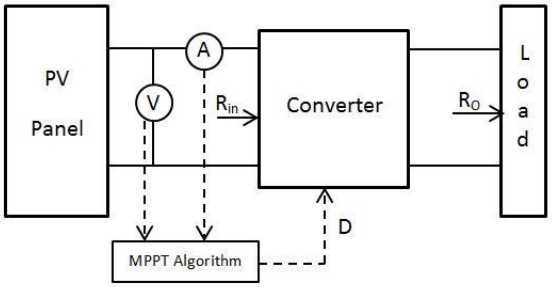

Fig. 2. The overall structure of a load-related PV system.

Figure 2 shows the overall structure of a load-related PV system. R_{in} is the internal resistance of the converter and R_O is the external resistance or load resistance. Equation 1 shows the relationship between R_{in} and R_O. R_O can be matched online with the R_{in}.

$$R_O = \left(D/1-D\right)^2 R_{in} \quad (2)$$

Many MPPT methods have been developed and implemented. The methods vary in complexity, sensors required, convergence speed, cost, range of effectiveness, implementation hardware, popularity, and other respects [14]. Through various methods, the most popular one is Perturb and Observe.

The P&O method is popular for its low cost, simple implementation, and little maintenance. It is performed based on comparing the power of two points after perturbation. Figure 3 shows the classical P&O algorithm in detail. According to the flowchart, the first step is to measure the instantaneous PV voltage and current and multiply them to get the instantaneous power. Then it compares the PV power with that of the previous cycle of perturbation. When PV power and PV voltage increase simultaneously or when PV power and PV voltage decrease simultaneously; a perturbation step size; ΔD will be added to the duty cycle; D; generates the next cycle of perturbation to force the operating point to

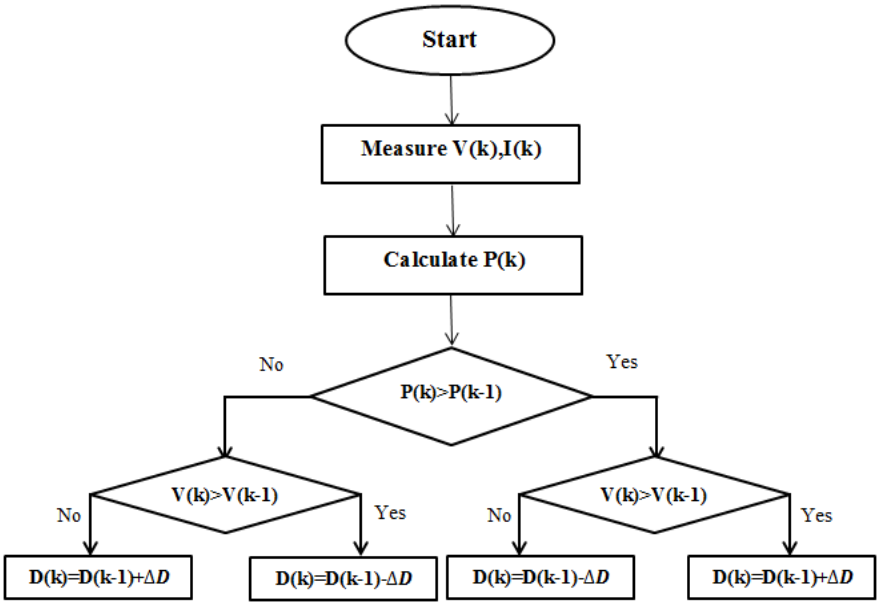

Fig. 3. Flowchart of perturb and observe method [12].

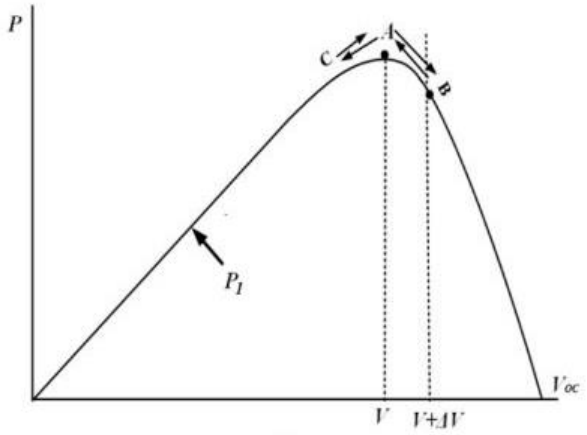

Fig. 4. MPPT oscillating around MPP [5].

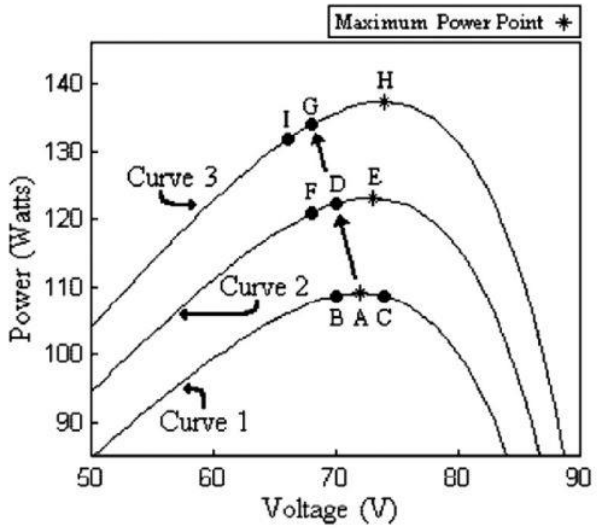

Fig. 5. Illustration of the erratic behaviour of P&O under rapidly increasing irradiance [14].

move towards the MPP. When PV power increases and PV voltage decreases simultaneously or when PV power decreases and PV voltage increases simultaneously, the perturbation step will be subtracted for the next cycle of perturbation [14, 15].

The advantages of the P&O algorithm are stated before but it has some drawbacks that reduce its MPPT efficiency.

The flowchart of this algorithm reveals that the perturbation is applied repeatedly during every sampling event and therefore the system oscillates around MPP throughout this process as shown in Figure 4. And this will result in loss of energy. Although by minimizing the perturbation step size (ΔD), the magnitude of oscillation can be reduced but it causes a reduction in the speed of MPP tracking [5]. The classical P&O method cannot determine when it actually reaches the MPP. Instead, it oscillates around the MPP and creates a fundamental drawback of classical P&O under rapidly changing irradiance levels. Consider the case in which the irradiance is such that it generates P–V curve 1 in Figure 5. The MPPT is oscillating

around the MPP from point B to A to C to A and so on. Then, assume the irradiance increases and the P–V curve of the array moves to curve 2. If during the rapid increase in solar irradiance and output power, the MPPT was perturbing the operating point from point A to point B, the MPPT would actually move from A to D. As shown in Fig5, this causes to increase in output power, and the MPPT will continue perturbing in the same direction, toward point F. If the irradiance is still rapidly increasing, the PV power curve will move to G on curve 3 instead of to F on curve 2. Again the MPPT will see a positive ΔP and will assume it is moving toward the MPP, continuing to perturb to point I. From points A to D to G to I the MPPT is continually moving away from the MPP (point H in curve 3), decreasing the efficiency of the P&O algorithm [5, 14].

Figure 6 shows the success and failure of the classical P&O method when the initial operating point lies to the right or left of MPP under increasing irradiation and constant temperature condition considering the size of ΔD[11].

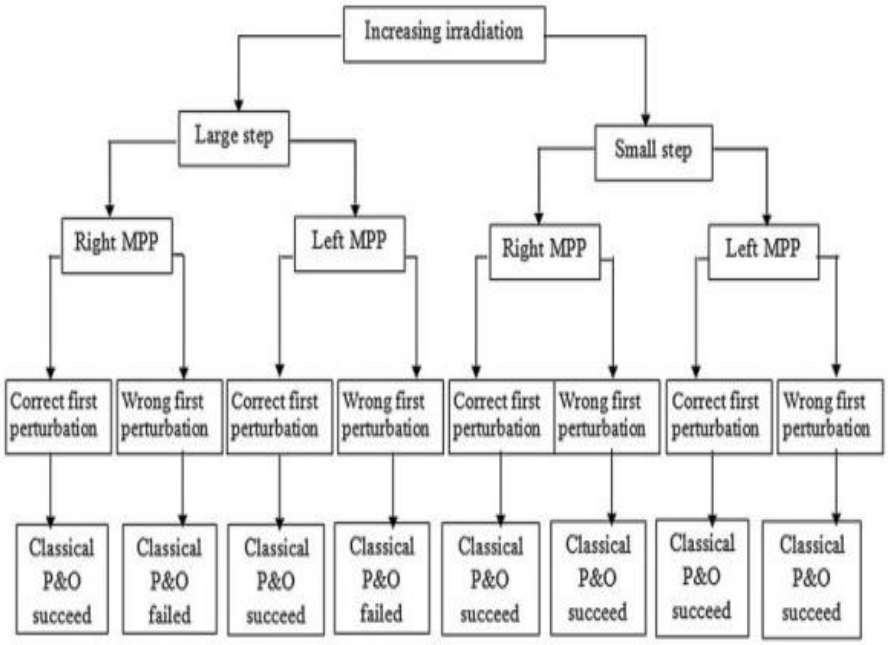

Fig. 6. Performance of the classical P&O method under increasing irradiation level [11].

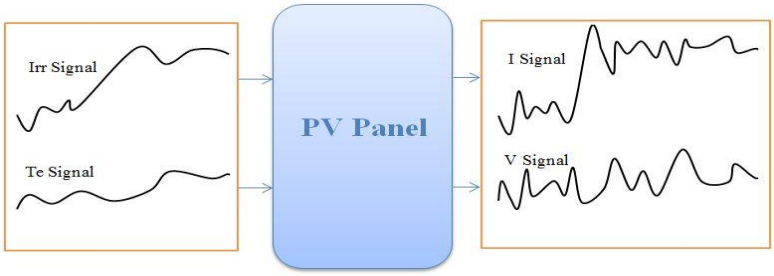

Fig. 7. An illustrative example of the process of mixing signals by PV panel.

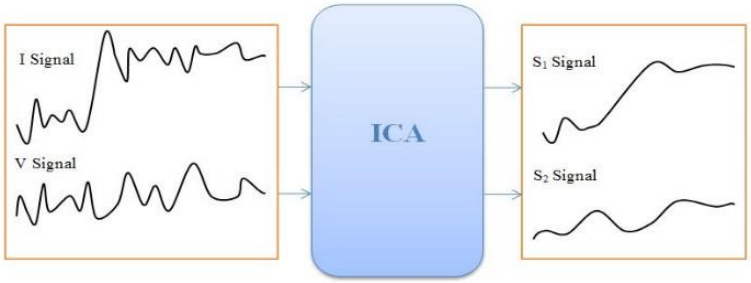

Fig. 8. An illustrative example of the process of extracting signals by ICA.

3. THE INDEPENDENT COMPONENT ANALYSIS CONCEPT AND ALGORITHM

Independent component analysis (ICA) is a widely-used blind source separation technique that can be obtained to decrease the drawback of the classical P&O method which is described in section 2.

In Figure 7 Two source signals (Irr and Te) are mixed linearly to form two new mixture signals (I and V) by the PV panel. The goal is to extract the original signals from mixtures of signals.

Figure 8 shows the process of extracting signals. S_1 and S_2 are the estimated of two source signals; Irr and Te; that are extracted from two mixture signals; I and V. Figure 8 shows that the S_1 and S_2 track the Irr and Te better than I and V therefore they can be obtained to determine whether the irradiation is increasing or decreasing to solve the problem of continually moving away from MPP.

The goal of the ICA algorithm is to find m ICs in K^{th} the sample (element of $s(K)$, namely IC vector) as sources from the m measured variables that are sampled from the sensors, CT or PT (element of $x(K)$, namely observed vector) [16, 17]. In principle, this method searches to find the unknown mixing matrix A and IC matrix S, from the known observed matrix X, where:

$$X = AS \tag{3}$$

Equation (3) can be rewritten as $\mathbf{S = W.X}$, where $\mathbf{W = A^{-1}}$. Matrix $\mathbf{X}$ is whitened using the whitening matrix $\mathbf{Q}$. The Matrix $\mathbf{Q}$ can be calculated as $\mathbf{Q = \Lambda^{\frac{-1}{2}} U^T}$ where A is a diagonal matrix with the eigenvalues of the matrix $\mathbf{R_x}$ as its diagonal elements and $\mathbf{U}$ is a matrix with corresponding eigenvectors of $\mathbf{R_x}$ as its columns, where $\mathbf{R_x} = E(\mathbf{x(k)x(k)}^T)$. The whitened matrix $\mathbf{Z}$ can be written as:

$$Z = QX = QAS = BS \tag{4}$$

According to literature [18], $\mathbf{B^{-1} = B^T}$. Therefore, the problem of finding a full rank matrix $\mathbf{A}$ is reduced to finding an orthogonal matrix $\mathbf{B}$. Equation (4) can be rewritten as $\mathbf{S = B}^T\mathbf{Z}$. It is a matrix equation with two unknown matrices $\mathbf{S}$ and $\mathbf{B}$ with two constraints; $\mathbf{B}$ is an orthonormal matrix [19] and the statistical dependence between elements $\mathbf{s(k)}$ should be minimized. Literature [19] offers a solution to this constraint optimization problem and suggests the Fast ICA (FICA) algorithm. This algorithm is explained by the following steps:

Step 1: Choose m (the dimension of the IC vector) and set the counter $i=1$

Step 2: Choose a random initial vector $\mathbf{b}_i$ with the unit norm, $\mathbf{b}_i$ which is a column of the matrix $\mathbf{B}$.

Step 3: Calculate

$$b_i \leftarrow E\left\{z\, G^{\bullet}\left(b_i^T\, z\right)\right\} - E\left\{G^{\bullet\bullet}\left(b_i^T\, z\right)\right\} b_i \qquad (5)$$

where $G^{\bullet}$ and $G^{\bullet\bullet}$ are the first and second derivatives of G. The Function $G(\mathbf{b}_i^T \mathbf{z})$ is defined as $\tanh(\mathbf{b}_i^T \mathbf{z})$ or $-\exp(-(\mathbf{b}_i^T \mathbf{z})^2/2)$, etc. G is any non-quadratic function proposed by [20] to approximate the negentropy and is well explained in it.

Step 4: Orthogonalize $\mathbf{b}_i$ using the Gram-Schmidt method:

$$b_i \leftarrow b_i - \sum_{j=1}^{i-1}\left(b_j^T\, b_i\right) b_j \qquad (6)$$

Step 5: Normalize $\mathbf{b}_i$ as:

$$b_i \leftarrow b_i / b_i \qquad (7)$$

Step 6: If $\mathbf{b}_i$ has not converged, go back to step 3. $\mathbf{b}_i$ is converged if the dot-product of old and new $\mathbf{b}_i$ is equal to around 1.

Step 7: If $\mathbf{b}_i$ has converged, it is i^{th} the vector of $\mathbf{B}$. Then, if $i < m$ set $i = i+1$ and go back to step 2.

To summarize, the matrix $\mathbf{B}$ is determined by the above-mentioned method. The IC matrix, $\mathbf{S}$, then is calculated as $\mathbf{S} = \mathbf{B}^T \mathbf{Z}$, and finally the de-mixing matrix, $\mathbf{W}$, is calculated as:

$$W = B^T Q \qquad (8)$$

4. THE PROPOSED METHOD

As shown in Figure 5, under constant temperature and rapidly increasing irradiance conditions, classical P&O has erratic behavior. The increase in power is due to an increase in irradiation which classical P&O cannot detect and also further away from MPP in each step. Adding an irradiation sensor eliminates one of the biggest advantages of P&O, which is its low cost. But With the help of ICA without the need for an irradiation sensor, the signal of irradiation changes is estimated and helps the classical P&O to have better performance. In general, this procedure is summarized in two main steps. In the first step, irradiation signal changes are estimated using the ICA algorithm and in the second step by using this estimated irradiation signal and voltage and current signals of the panel, a proposed method is provided based on the P&O algorithm to improve classical P&O weakness in rapidly changing irradiation conditions. Finally, the output of this algorithm is used to generate pulses in the boost converter.

4.1. Estimate Irradiation Signal Changes

Pointing out that the current and voltage of the panel are influenced by the intensity of irradiation and ambient temperature. In the proposed method, the voltage and current of the panel enter the ICA block as ICA inputs, and the ICA algorithm is implemented on them. Finally, the estimated source signals are obtained to illustrate the changes in the irradiation signal; Irr; and the panel surface

temperature; Te. With a reminder of the fact that the simulation was performed under constant temperature condition, only the irradiation signal changes are used to continue work.

The achieved irradiation signal changes consist of two parts: an offline part is carried out to identify the initial simple model of the panel and an online part is carried out to update this model and estimate the source signals (irradiation signal); Irr; and the panel temperature; Te. These two parts are explained as follows:

4.1.1. The Offline Part

The steps of the offline part are described as follows:

Step 1: Choose N>10 (samples number of output current and voltage of panel in a condition that the temperature and irradiation are constant)

Step 2: Construct the Observation matrix X, $X = X(K)\ K = 1,\ldots,N$, where vector $\mathbf{X}(k) = \begin{bmatrix} x_{1k} \\ x_{2k} \end{bmatrix}$ and x_{1k} is k-th sample of PV panel current and x_{2k} is k-th sample of PV panel voltage.

Step 3: $\mathbf{X}$ should be normalized using the mean and standard deviation of each row.

Step 4: Compute the whitened matrix $\mathbf{Z}$ by Equation (3).

Step 5: Perform the ICA algorithm to obtain matrix $\mathbf{B}$, matrix **S,** and matrix $\mathbf{A}$ (initial model of the panel) by step 1 to step 7 of the ICA algorithm (see section 3). In ICA algorithm $m = 2$ is chosen.

Step 6: Obtain the $\Delta\mathbf{S} = \mathbf{S}(k) - \mathbf{S}(k-1)$ k=1,…, N, and calculate the variance of each row of matrix $\Delta\mathbf{S}$; δ_1 and δ_2; then determine the $\delta = Max\{\delta_1, \delta_2\}$.

4.1.2. The Online Part

The steps of the online part are described as follows:

Step1: Construct the Observation vector $\mathbf{X}(k+1)$, where vector $\mathbf{X}(k+1) = \begin{bmatrix} x_{1k+1} \\ x_{2k+1} \end{bmatrix}$ and x_{1k+1} is k+1-th sample of PV panel current and x_{2k+1} is k+1-th sample of PV panel voltage.

Step 2: Calculate the $\mathbf{Z}(k+1) = \mathbf{Q}\mathbf{X}(k+1)$

Step 3: Reconstruct the Observation matrix $\mathbf{X}$ by $\mathbf{X}(k) = \mathbf{X}(k+1) \quad k = 1,\ldots,N$.

Step 4: $\mathbf{x}_K$ should be normalized using the mean and standard deviation of each row.

Step 5: Recalculate $\mathbf{Q}$ and the whitened matrix $\mathbf{Z}$ by Equation (2) (see section 3).

Step 6: Perform the ICA algorithm to obtain the new matrix $\mathbf{B}$ and matrix $\mathbf{A}$ (update model of the panel) by step 1 to step 7 of the ICA algorithm (see section 3). In ICA algorithm $m = 2$ is chosen.

Step 7: Go back to Step 1

To summarize, the vector $\mathbf{S}(k+1) = \begin{bmatrix} s_{1k+1} \\ s_{2k+1} \end{bmatrix}$ is determined by the above-mentioned method.

In practice, the temperature variation is smooth therefore the row of the vector **S** is not smooth which shows an estimation of the irradiation signal. As a result, the estimation of irradiation change; ΔIrr; can be estimated by $\tilde{\Delta Irr} = Max\{s_{1k+1} - s_{1k}, s_{2k+1} - s_{2k}\}$.

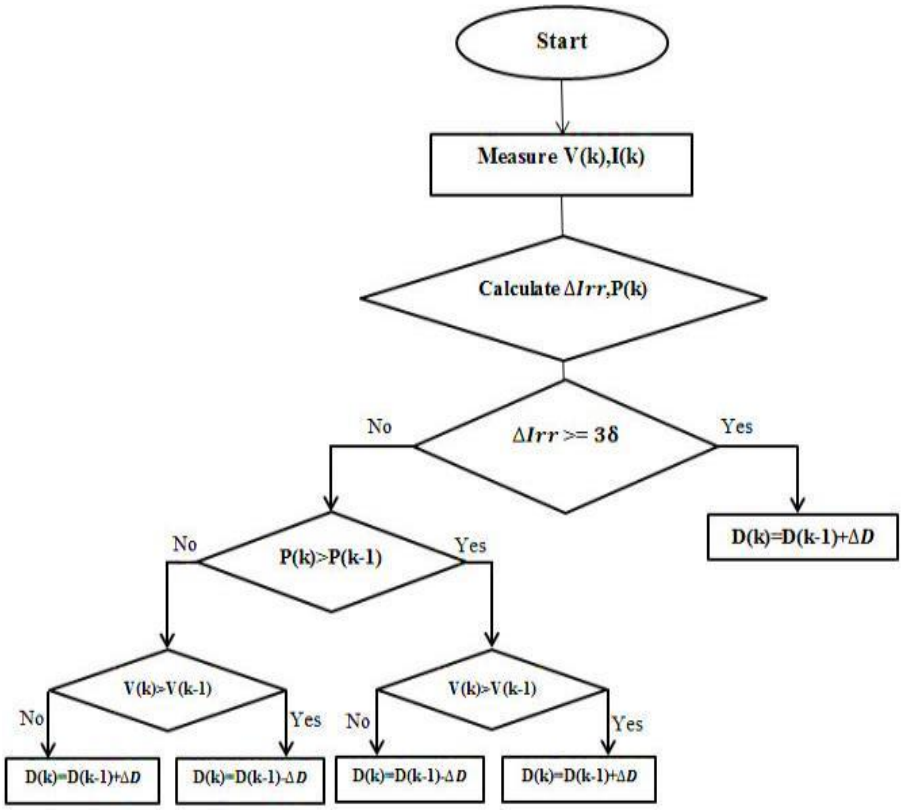

Fig .9. The proposed method algorithm.

4.2. The Proposed Algorithm

In continuation with the availability of irradiation signal, MPPT in addition to checking the values of voltage and power also can consider the process of irradiation changes and then decide whether to increase or decrease the value of D unless the mistake mentioned in classical P&O occurs. Figure 9 shows the maximum power point tracking algorithm using the proposed method. V and I are the voltage and current of the panel respectively and ΔIrr shows an estimation of irradiation change. Figure 9 shows the proposed algorithm is similar to the classical P&O algorithm unless when ΔIrr is bigger than a threshold level. The threshold level is assumed 3δ where the δ is a variance of estimation of irradiation change under normal panel operating conditions (when the irradiation is constant). It is calculated from the step 6 of the offline part. It is worth mentioning that it is assumed a normal distribution for irradiation under normal panel operating conditions also the mean of signal is zero.

The variance of the irradiation (δ), is calculated from the third step of the offline section. P is the output power of the panel that is calculated as $\boldsymbol{V}.\boldsymbol{I}$; D; is the duty coefficient of the boost converter. As mentioned before, this simulation was performed in constant temperature and rapidly increasing irradiation condition, so as the irradiation

increases, the MPP moves to the right, and at each step, D must increase by ΔD . But if ΔIrr is smaller than 3δ the conventional P&O is executed.

5. SIMULATION

The algorithm shown in Figure 9 is coded in MATLAB function block and its output is used to generate boost converter pulses.

The simulations were performed in two different ways to compare the performance of the classical P&O method and the proposed method in similar conditions. The table below shows the datasheet parameter values of the PV module used in this paper. Current-voltage and power-voltage characteristics of the PV module are illustrated in Figure 10 and Figure 11 respectively.

Table 1. ***The Datasheet parameter value of the PV module.***

Trina-Solar TSM-250PA05.08	
Maximum Power (W)	249.86
Open Circuit Voltage V_{OC} (V)	37.6
Short Circuit Current I_{SC} (A)	8.55
Voltage at maximum power point V_{mp} (V)	31
Current at maximum power point I_{mp} (A)	8.06
Shunt resistance R_{sh} (Ohms)	301.849
Series Resistance R_s (Ohms)	0.247

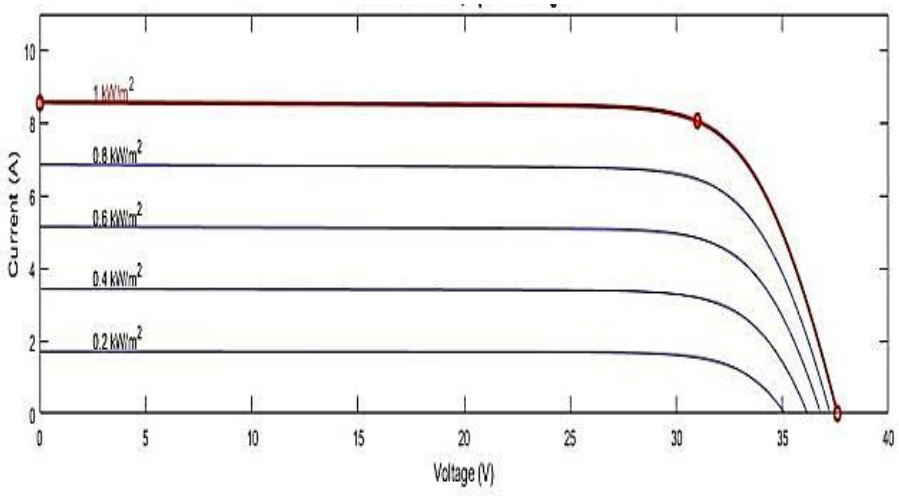

Fig. 10. Current-voltage characteristics of the PV module.

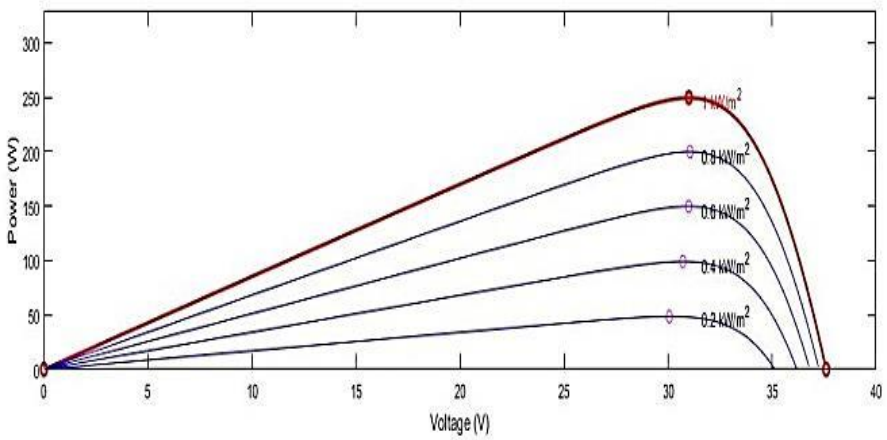

Fig. 11. power-voltage characteristics of the PV module.

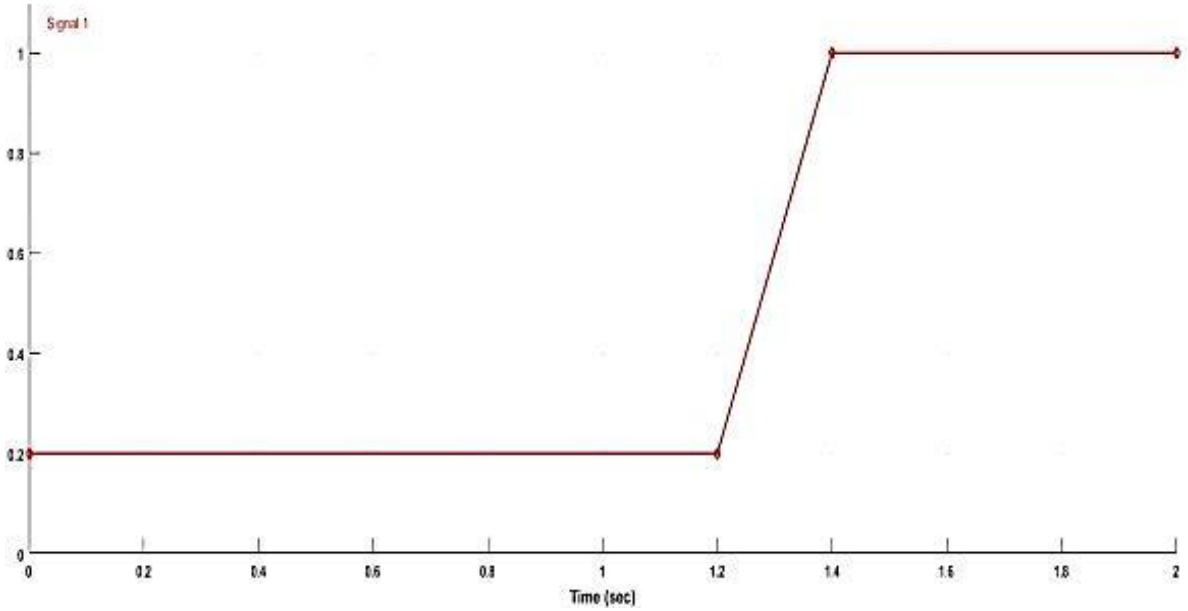

Fig. 12. The input irradiation signal.

In simulations, the ambient temperature is constant (25℃), and the irradiation signal is shown in Figure 12. The offline part of the proposed algorithm is run at the first second and the online part is run after 1 second. In Figure 12, the irradiation signal increases from 1.2 s to 1.4 s and remains constant after that.

It is noteworthy that in this simulation, along with the voltage and current signals, the noise signal that is always present in the environment enters the ICA block, which will bring the result closer to reality. The input noise specifications are given in table 2.

Table 2. ***The input noise specifications*****.**

Input Noise	
Noise	Band-Limited white noise
Noise Power	0.00001
Sample Time	0.0001

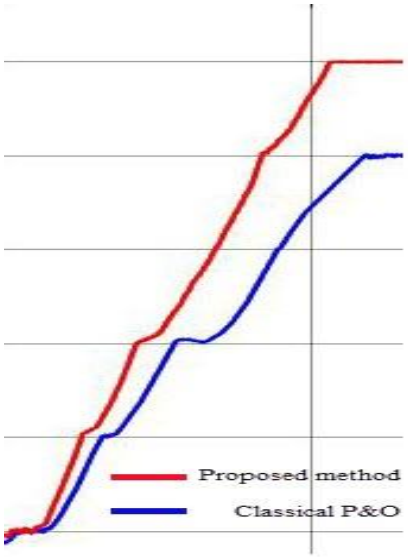

Fig. 13. Comparison of the controller duty coefficient (D) changes.

Table 3. ***The average output power.***

Method	Average of output power
Classical P&O	51.53
Proposed method	53.77

Simulation results show that the performances of both methods are similar under constant irradiation, but from t=1.2 with increasing the irradiation, the proposed method performed better than the classical P&O method because of applying estimation of irradiation change. Figure 13 shows the comparison of the controller duty coefficient (D) changes in transient time. As shown in figure 13, the duty coefficient D of the proposed method is completely ascending in the period of irradiation increase, as expected.

The simulation is repeated 10 times and the average output power in each method is shown in Table 3.

Figure 14 illustrates the output power curves taken from the panel. When the temperature and irradiation are constant, the algorithms behave similarly, so the blue and red graphs overlap, and the parts of the blue graph below the red graph are not visible in the figure. During the irradiation increase period, the proposed method receives more output power from the panel.

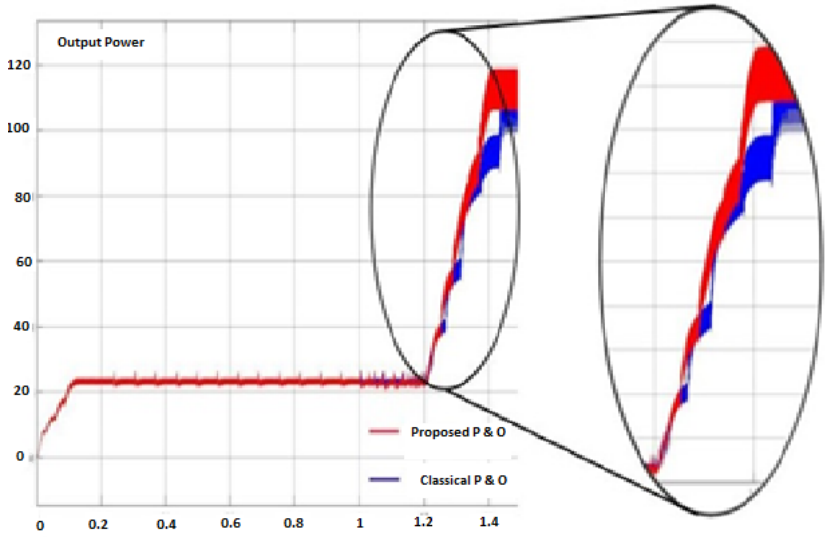

Fig. 14. Illustrated the output power curves taken from the panel.

Table 4. ***Comparison of the results of the two methods by changing the irradiation signal.***

Irradiation increase time	Duration of irradiation increase	Mean of power		Rise time	
		Classical P&O	Proposed P&O	Classical P&O	Proposed P&O
1.5-1.55	0.05	40.74	42.54	0.198	0.129
1.3-1.4	0.1	48.74	50.95	0.203	0.137
1.2-1.35	0.15	52.29	54.72	0.225	0.154
1.2-1.4	0.2	51.53	53.77	0.247	0.205
1.2-1.5	0.3	49.73	51.61	0.32	0.3
1.2-1.6	0.4	47.7	49.37	0.404	0.4
1.1-1.6	0.5	49.9	51.6	0. 505	0.5
1.1-1.7	0.6	47.82	49.29	0.605	0.6
1.7-1.8	0.7	45.74	46.98	0.696	0.693
1.05-1.85	0.8	45.77	46.95	0.802	0.799
Average		47.996	49.778	0.421	0.392

For more investigation, some factors of the classical P&O method and the proposed method by change in duration irradiation time, change in starting point (D_0), and change in step for increasing or decreasing D (ΔD) parameters were compared. The simulations are run at constant temperature and fast increasing irradiation, which are the assumed conditions of the article.

5.1. Change in Duration Irradiation Time

The duration of irradiation increase is assumed to be a variable factor (Δt). The initial irradiation is 200, which reaches 1000 after the Δt seconds. Simulations were performed for 10 different Δts.

Table 4 shows the performance of the proposed method is better than the classic method. In other words, the average mean power increases about 4%, and the average of rise time decreases about 7%.

5.2. Change in Starting Point (D_0)

Another influential factor in the P&O method is the starting point of D. To ensure the performance of this method, the simulation was performed with 5 different starting points.

Table 5 shows that this method is not dependent on the starting point and has a better performance, and the average mean power increases about 4% and the average of rise time decreases about 20%.

5.3. Change in Sep for Increasing or Decreasing D (ΔD)

The amount of ΔD, which is an important factor in the speed to reach MPP if the correct direction is detected and also effective in the amount of fluctuations in P&O, was assumed to be a variable factor. The results of the simulation of the proposed algorithm and classical P&O with different ΔD below were examined. Table 6 shows that the performance of the proposed method is better than the classic method. In other words, the average mean power increases about 4% and the average rise time decreases about 17%.

5.4. A Brief Comparison Between Proposed P & O And the Method Proposed by [13]

The method proposed by reference [13] is simulated and compared with the proposed method, both methods improve output power in comparison to the classic method but there isn't a meaningful difference between these two methods in output power.

Table 5. ***Comparison of the results of the two methods by changing D0.***

D_0	Mean of power		Rise time	
	Classical P&O	Proposed method	Classical P&O	Proposed method
0.3	51.83	54.04	0.25	0.204
0.4	51.7	53.9	0.25	0.204
0.5	51.53	53.77	0.25	0.205
0.6	51.3	53.49	0.248	0.205
0.7	51.04	53.24	0.249	0.206
Average	51.48	53.688	0.2494	0.2046

Table 6. ***Comparison of the results of the two methods by changing*** ΔD **.**

ΔD	Mean of power		Rise time	
	Classical P&O	Proposed method	Classical P&O	Proposed method
0.0002	49.81	52.61	0.349	0.24
0.00035	51.53	53.77	0.248	0.205
0.0005	52.04	53.96	0.212	0.205
0.0007	52.24	54.06	0.225	0.205
0.001	52.37	54.08	0.213	0.205
Average	51.598	53.696	0.2494	0.212

6. CONCLUSION

Efforts have been made to achieve greater power from solar panels. And so far many different methods have been proposed to improve MPP tracking. The concern of many researchers is to improve the performance of the existing methods. In this paper, the aim is to improve the performance of the P&O method under constant temperature conditions and the fast increase of irradiation that the classic P&O fails to track the MPP. For this purpose, the ICA algorithm was used and by implementing this algorithm, changes in the irradiation signal were obtained without the use of an irradiation sensor. Using this signal in writing the new algorithm reduced the required time to get around MPP and more importantly, increased the average output power. In order to illustrate the improved performance of the proposed method in different conditions, the irradiation increase times are changed between 1.05 to 1.85 seconds and it is shown that the output power mean increases and rise time decreases in the proposed P&O compared to the classic P&O. Also the starting point (D0) is changed between 0.3 to 0.7, in all simulations the output power mean increases and rise time decreases in the proposed P&O compared to classic P&O. finally, 5 values are chosen as steps for increasing or decreasing D (ΔD). In all the 5 simulations, the output power mean increases and rise time decreases in the proposed P&O compared to classic P&O.

It is worth mentioning that due to the addition of computational operations in the proposed method, the execution time of this method is longer than the classical P&O method. Of course, with the growing trend of equipment in various parts of hardware and software, this problem will be negligible.

REFERENCES

[1] Venkateswari R., Sreejith S. (2019) Factors influencing the efficiency of photovoltaic system. Renewable and Sustainable Energy Reviews, vol. 101, pp. 376-394.

[2] Reisi A. R., Moradi M. H., Jamasb S.(2013) Classification and compa rison of maximum power point tracking techniques for photovoltaic system. Renewable and Sustainable Energy Reviews, vol. 19, pp. 433-443.

[3] Bounechba H., Bouzid A., Snani H., Lashab A.(2016) Real time simulation of MPPT algorithms for PV energy system. Electrical Power and Energy System, vol. 83, pp. 67-78.

[4] Pilakkat D., Kanthalakshmi S. (2019). An improved P&O algorithm integrated with artificial bee colony for photovoltaic systems under partial shading conditions. Sol. Energy, vol. 178, pp. 37-47.

[5] Ahmad R., Murtaza A. F., Sher H. A. (2019) Power tracking techniques for efficient operation of photovoltaic array in solar applications. Renewable and Sustainable Energy Reviews, vol. 101, pp. 82-102.

[6] Rezk H., et al. (2019). A novel statistical performance evaluation of most modern optimization based global MPPT techniques for partially shaded PV system. Renewable and Sustainable Energy Reviews, vol. 115, pp. 109372.

[7] Yilmaz U., Turksoy O., Teke A. (2019)

Improved MPPT method to increase accuracy and speed in photovoltaic systems under variable atmospheric conditions. Electrical Power and Energy System, vol. 113, pp. 634-651.

[8] Feroz Mirza A. et al. (2019), Novel MPPT techniques for photovoltaic systems under uniform irradiance and Partial shading. Sol. Energy, vol. 184, pp. 628-648.

[9] Alik R., Jusoh A. (2017). Modified Perturb and Observe (P&O) with checking algorithm under various solar irradiation. Sol. Energy, vol. 148, pp. 128-139.

[10] Killi, M., Samanta, S. (2015) Modified perturb and observe MPPT algorithm for drift avoidance in photovoltaic systems. IEEE Trans. Indus. Electron, vol. 3, no.2, pp. 1 –10.

[11] Kamala, V., Premkumar, K., Bisharathu, A., Ramaiyer, S. A. (2017) modified Perturb & Observe MPPT technique to tackle steady state and rapidly varying atmospheric conditions'. Sol. Energy, vol. 157, pp. 419 –426.

[12] Abdalla, I., Zhang, L., Corda, J. (2011) Voltage-hold Perturbation & Observation maximum power point tracking algorithm (VH-P&O MPPT) for improved tracking over the transient atmospheric changes. In: Proc. Conf. Power Electronics and Applications, Birmingham, United Kingdom; pp. 1 – 10.

[13] Abdel-Salam M. et al. (2018). An improved perturb-and-observe based MPPT method for PV systems under varying irradiation levels. Sol. Energy, vol. 171, pp. 547-561.

[14] Eltawil M. A., Zhao Z. (2013) MPPT techniques for photovoltaic applications. Renewable and Sustainable Energy Reviews, vol. 25, pp. 793-813.

[15] Kota V. R., Bhukya M. N. (2016). A novel linear tangents based P & O scheme for MPPT of a PV system. Renewable and Sustainable Energy Reviews;

[16] Teimoortashloo M., Khadi Sedigh A., (2018). A Dynamic Independent Component Analysis Approach to Fault Detection with New Statistics. Comput. Syst. Sci. Eng, vol. 33, no. 1.

[17] Teimoortashloo, M., Khaki Sedigh, A. (2015). A Modified Independent Component Analysis-Based Fault Detection Method in Plant-wide Systems. *Control and cybernetics*, vol. 44, no. 2, pp. 287-310.

[18] Lee, J.M., Yoo, C.K. and Lee, I.B. (2004). Statistical Process Monitoring with Independent Component Analysis. *Journal of Process Control*, vol. 14, no. 5, pp. 467–485

[19] Hyvarinen, A., Karhunen, J. and Oja, E. (2001). Independent Component Analysis. New York: John Wiley & Sons, ISBN 0-471-22131-7.

[20] Hyvarinen, A. (1999). Fast and Robust Fixed-point Algorithms for Independent component Analysis. *IEEE Trans. on Neural Networks*, vol. 10, no. 3, pp. 626–634.